# Technical Note on CERES EBAF Ed2.6
# TOA Outgoing Clear-Sky Shortwave Radiation (rsutcs)

## 1. Intent of This Document and POC

**1a)** This document is intended for users who wish to compare satellite derived observations with climate model output in the context of the CMIP5/IPCC historical experiments. Users are not expected to be experts in satellite derived Earth system observational data. This document summarizes essential information needed for comparing this dataset to climate model output. References are provided at the end of this document to additional information.

This NASA dataset is provided as part of an experimental activity to increase the usability of NASA satellite observational data for the modeling and model analysis communities. This is not a standard NASA satellite instrument product, but does represent an effort on behalf of data experts to identify a product that is appropriate for routine model evaluation. The data may have been reprocessed, reformatted, or created solely for comparisons with climate model output. Community feedback to improve and validate the dataset for modeling usage is appreciated. Email comments to HQ-CLIMATE-OBS@mail.nasa.gov .

Dataset File Name (as it appears on the ESG):

rsutcs_CERES-EBAF_L4_Ed2-6_200003-201012.nc

**1b)** Technical point of contact for this dataset:

Norman Loeb email:Norman.g.loeb@nasa.gov

## 2. Data Field Description

| | |
|---|---|
| CF variable name, units: | TOA Outgoing Clear-Sky Shortwave Radiation (rsutcs), $Wm^{-2}$ |
| Spatial resolution: | 1°x1° latitude by longitude |
| Temporal resolution and extent: | Monthly averaged from 03/2000 to 12/2010 |
| Coverage: | Global |

## 3. Data Origin

CERES instruments fly on the Terra (descending sun-synchronous orbit with an equator crossing time of 10:30 A.M. local time) and Aqua (ascending sun-synchronous orbit with an equator crossing time of 1:30 P.M. local time) satellites. Each CERES instrument measures filtered radiances in the shortwave (SW; wavelengths between 0.3 and 5 μm), total (TOT; wavelengths between 0.3 and 200 μm), and window (WN; wavelengths between 8 and 12 μm) regions. To correct for the imperfect spectral response of the instrument, the filtered radiances are converted to unfiltered reflected solar, unfiltered emitted terrestrial longwave (LW) and window (WN) radiances (Loeb et al. 2001). Since there is no LW channel on CERES, LW daytime radiances are determined from the difference between the TOT and SW channel radiances. Instantaneous top-of-atmosphere (TOA) radiative fluxes are estimated from unfiltered radiances using empirical angular distribution models (ADMs; Loeb et al. 2003, 2005) for scene types identified

using retrievals from Moderate Resolution Imaging Spectrometer (MODIS) measurements (Minnis et al. 2011). Monthly mean fluxes are determined by spatially averaging the instantaneous values on a 1º×1º grid, temporally interpolating between observed values at 1-h increments for each hour of every month, and then averaging all hour boxes in a month. Level-3 processing is performed on a nested grid, which uses 1° equal-angle regions between 45°N and 45°S, and maintains area consistency at higher latitudes. The fluxes are then output to a complete 360x180 1°×1° grid created by replication.

Monthly regional CERES clear-sky SW TOA fluxes in the CMIP5 archive are from the CERES Energy Balanced and Filled (EBAF) Ed2.6 data product. The approach used to determine clear-sky SW TOA flux is described in detail in Loeb et al. (2009). We determine gridbox mean clear-sky fluxes using an area-weighted average of: (i) CERES/Terra broadband fluxes from completely cloud-free CERES footprints (20-km equivalent diameter at nadir), and (ii) MODIS/Terra-derived ‘‘broadband’’ clear-sky fluxes estimated from the cloud-free portions of partly and mostly cloudy CERES footprints. In both cases, clear regions are identified using the CERES cloud algorithm applied to MODIS pixel data (Minnis et al. 2011). Clear-sky fluxes in partly and mostly cloudy CERES footprints are derived using MODIS–CERES narrow-to-broadband regressions to convert MODIS narrowband radiances averaged over the clear portions of footprints to broadband SW radiances. The narrow-to-broadband regressions applied to MODIS are developed independently for each month in order to ensure that the final product’s calibration is tied to CERES. The ‘‘broadband’’ MODIS radiances are then converted to TOA radiative fluxes using CERES clear-sky ADMs (Loeb et al. 2005). Monthly mean clear-sky TOA fluxes are determined from instantaneous values using the same approach as clear-sky fluxes in the CERES SSF1deg product. In that product, SW radiative fluxes between CERES observation times are determined from the observed fluxes by using scene-dependent diurnal albedo models, which describe how TOA albedo (and therefore flux) changes with solar zenith angle for each local time, assuming the scene properties remain invariant throughout the day. The sun angle–dependent diurnal albedo models are based upon the CERES ADMs developed for the Tropical Rainfall Measuring Mission (TRMM) satellite (Loeb et al. 2003).

## 4. Validation and Uncertainty Estimate

Regional monthly mean SW clear-sky TOA fluxes are derived from Level-1 and -2 data. The Level-1 data correspond to calibrated radiances. Here we use the latest CERES gains and time-dependent spectral response function values (Thomas et al., 2010, Loeb et al., 2011). The Level-2 TOA fluxes are instantaneous values at the CERES footprint scale. Their accuracy has been evaluated in several articles (Loeb et al., 2006; Loeb et al., 2007; Kato and Loeb, 2005).

Figs. 1a and 1b provide regional plots of mean clear-sky SW TOA flux and interannual variability for the month of March based upon all March months between 2000 and 2010. The regional 1°x1° standard deviation ranges from near zero over remote ocean regions to 35 $Wm^{-2}$ over mid-latitude land regions, associated with seasonal snow. Considering all 1°x1° regions, the overall global regional standard deviation in SW clear-sky TOA flux is 22 $Wm^{-2}$, and the overall global mean is 54 $Wm^{-2}$.

The uncertainty in 1°x1° regional SW clear-sky TOA flux is determined from calibration uncertainty, error in narrow-to-broadband conversion, ADM error, time-space averaging, and scene identification. For CERES, calibration uncertainty is 1% (1$\sigma$), which for a typical global

mean clear-sky SW flux corresponds to ≈0.5 $Wm^{-2}$. Figs. 2a and 2b show the regional distribution of the correction used to correct for regional narrow-to-broadband error. This is derived by applying narrow-to-broadband regressions to MODIS visible radiances for completely cloud-free CERES footprints and then comparing the estimated broadband flux with CERES. The overall bias is 0.2 $Wm^{-2}$ and the regional RMS difference is 0.65 $Wm^{-2}$. Assuming a 50% error in the correction, the narrowband-to-broadband contribution to regional uncertainty becomes 0.3 $Wm^{-2}$. For clear-sky SW TOA flux, ADM error contributes 1 $Wm^{-2}$ to regional RMS error (Loeb et al., 2007), and time-space averaging adds 2 $Wm^{-2}$ uncertainty. The latter is based upon an estimate of the error from TRMM-derived diurnal albedo models that provide albedo dependence upon scene type (Loeb et al., 2003). In EBAF, "clear-sky" is defined as cloud-free at the MODIS pixel scale (1 km). A pixel is identified as clear using spectral MODIS channel information and a cloud mask algorithm (Minnis et al., 2011). Based upon a comparison of SW TOA fluxes for CERES footprints identified as clear according to MODIS but cloudy according to CALIPSO, and TOA fluxes from footprints identified as clear according to both MODIS and CALIPSO, Sun et al. (2011) found that footprints with undetected subvisible clouds reflect 2.5 $Wm^{-2}$ more SW radiation compared to completely cloud-free footprints, and occur in approximately 50% of footprints identified as clear by MODIS. This implies an error of 1.25 $Wm^{-2}$ due to misclassification of clear scenes. The total error in TOA outgoing clear-sky SW radiation in a region is $\mathrm{sqrt}(0.5^2+0.3^2+1^2+2^2+1.25^2)$ or approximately 3 $Wm^{-2}$.

Table 1 compares global TOA averages for EBAF Ed2.6 with earlier versions EBAF Ed1.0 and EBAF Ed2.5. Clear-sky SW TOA flux in Ed2.6 is 0.3 $Wm^{-2}$ greater than Ed1.0 and 0.1-0.2 $Wm^{-2}$ greater than Ed2.5. The main difference between EBAF Ed2.6 and Ed2.5 is that Ed2.6 applies geodetic weighting when averaging globally while geocentric weighting is assumed in EBAF Ed2.5. In EBAF Ed1.0, geocentric weighting is assumed and the methodology for time-space averaging differs somewhat from Ed2.5 and Ed 2.6. Time-space averaging for the latter is now based upon the same code as is used for clear-sky SW TOA fluxes in the SSF1deg product.

Table 1 Global mean TOA fluxes from EBAF Ed1.0, EBAF Ed2.5 and EBAF Ed2.6 for March 2000–February 2005, March 2000–February 2010, and January 2006–December 2010.

| | March 2000–February 2005 | | |
|---|---|---|---|
| | EBAF Ed1.0 | EBAF Ed2.5 | EBAF Ed2.6 |
| Incoming Solar | 340.0 | 340.2 | 340.5 |
| LW (all-sky) | 239.6 | 239.6 | 239.9 |
| SW (all-sky) | 99.5 | 99.7 | 100.0 |
| Net (all-sky) | 0.85 | 0.85 | 0.55 |
| LW (clear-sky) | 269.1 | 266.2 | 266.5 |
| SW (clear-sky) | 52.9 | 52.4 | 52.6 |
| Net (clear-sky) | 18.0 | 21.5 | 21.4 |
| | March 2000–February 2010 | | |
| | EBAF Ed1.0 | EBAF Ed2.5 | EBAF Ed2.6 |
| Incoming Solar | | 340.1 | 340.4 |
| LW (all-sky) | | 239.6 | 239.9 |
| SW (all-sky) | | 99.5 | 99.9 |
| Net (all-sky) | | 1.0 | 0.59 |
| LW (clear-sky) | | 266.0 | 266.4 |
| SW (clear-sky) | | 52.4 | 52.5 |
| Net (clear-sky) | | 21.6 | 21.5 |
| | January 2006–December 2010 | | |
| | EBAF Ed1.0 | EBAF Ed2.5 | EBAF Ed2.6 |
| Incoming Solar | | | 340.3 |
| LW (all-sky) | | | 239.8 |
| SW (all-sky) | | | 99.9 |
| Net (all-sky) | | | 0.58 |
| LW (clear-sky) | | | 266.1 |
| SW (clear-sky) | | | 52.5 |
| Net (clear-sky) | | | 21.7 |

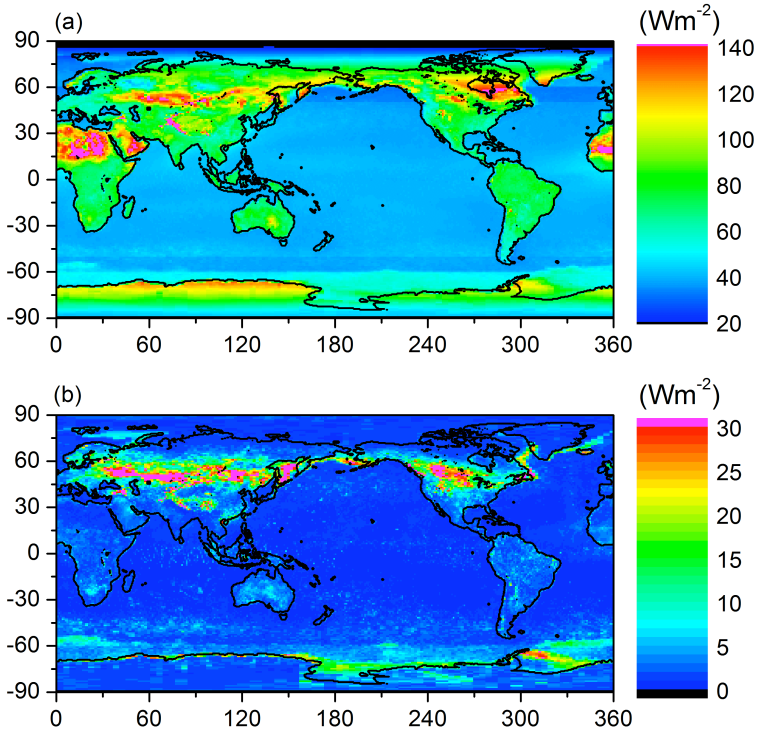


Figure 1 (a) Average and (b) standard deviation of SW clear-sky TOA flux determined from all March months from 2000–2010 using the CERES EBAF2.5B product.

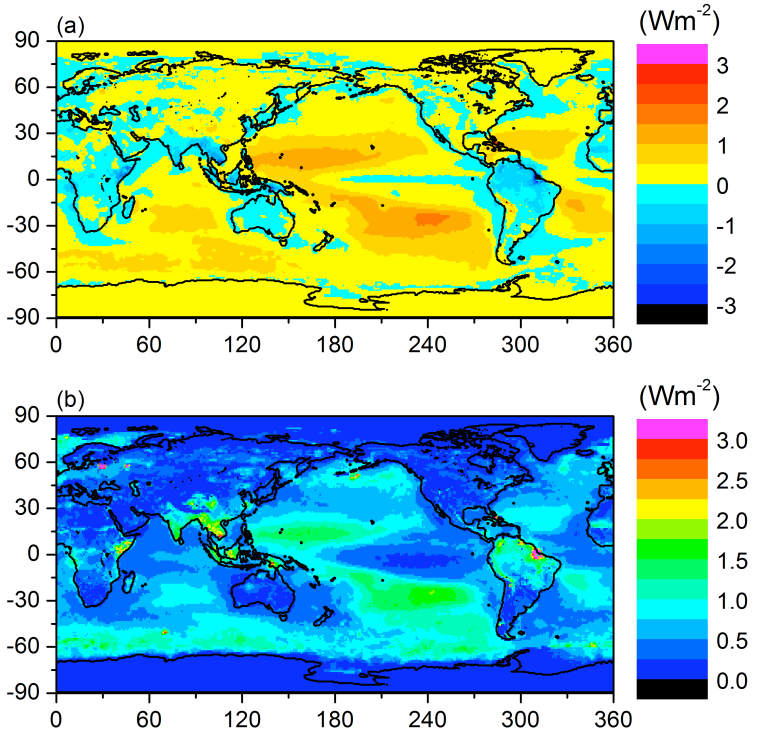


Figure 2 (a) Bias and (b) RMS difference between high-resolution TOA clear-sky fluxes derived with and without corrections for regional narrow-to-broadband error.

## 5. Considerations for Model-Observation Comparisons

Clear-sky TOA fluxes in EBAF Ed2.6 are provided for all MODIS pixels identified as clear at 1-km spatial resolution. This definition differs from what is used in the standard CERES data products (SSF1deg and SYN1deg), which only provide clear-sky fluxes in regions that are cloud-free at the CERES footprint scale. SW TOA fluxes for clear-sky regions identified at the higher spatial resolution are on average 1.6 $Wm^{-2}$ higher overall compared to the coarser resolution footprint case, and the monthly mean regional RMS difference is 6 $Wm^{-2}$. Users should be aware that both of these definitions for "clear-sky" might differ from what is used in climate model output. Many models compute clear-sky radiative fluxes in each column, regardless of whether the column is clear or cloudy. As a result, model-based clear-sky SW TOA fluxes may be biased high compared to the EBAF clear-sky SW observations.

Clear-sky monthly mean SW TOA fluxes are determined by inferring TOA fluxes at each hour of the month and averaging. TOA fluxes between observation times are determined from the observed fluxes by using scene-dependent diurnal albedo models to estimate how TOA albedo (and therefore flux) changes with solar zenith angle for each local time, assuming the scene properties remain invariant throughout the day. Therefore, we do not explicitly account for changes in the physical properties of the scene (e.g., aerosols, surface properties) during the coarse of the day. Since the CERES instruments provide global coverage daily, monthly mean regional fluxes are based upon complete daily samples over the entire globe.

When the solar zenith angle is greater than 90°, twilight flux (Kato and Loeb, 2003) is added to the outgoing SW flux in order to take into account the atmospheric refraction of light. The magnitude of this correction varies with latitude and season, and is determined independently for all-sky and clear-sky conditions. In general, the regional correction is less than 0.5 W $m^{-2}$ and the global mean correction is 0.2 W $m^{-2}$. Due to the contribution of twilight, there are regions near the terminator in which outgoing SW TOA flux can exceed the incoming solar radiation. Users should be aware that in these cases, albedos (derived from the ratio of outgoing SW to incoming solar radiation) exceed unity.

Since TOA flux represents a flow of radiant energy per unit area, and varies with distance from the earth according to the inverse-square law, a reference level is also needed to define satellite-based TOA fluxes. From theoretical radiative transfer calculations using a model that accounts for spherical geometry, the optimal reference level for defining TOA fluxes in radiation budget studies for the earth is estimated to be approximately 20 km. At this reference level, there is no need to explicitly account for horizontal transmission of solar radiation through the atmosphere in the earth radiation budget calculation. In this context, therefore, the 20-km reference level corresponds to the effective radiative ''top of atmosphere'' for the planet. Since climate models generally use a plane-parallel model approximation to estimate TOA fluxes and the earth radiation budget, they implicitly assume zero horizontal transmission of solar radiation in the radiation budget equation, and do not need to specify a flux reference level. By defining satellite-based TOA flux estimates at a 20-km flux reference level, comparisons with plane-parallel climate model calculations are simplified since there is no need to explicitly correct plane-parallel climate model fluxes for horizontal transmission of solar radiation through a finite earth. For a more detailed discussion of reference level, please see Loeb et al. (2002).

## 6. Instrument Overview

See the first paragraph of Section 3 for an overview of the CERES instruments on the Terra and Aqua satellites.

## 7. References

The full version of CERES EBAF Ed2.6 is available from the following ordering site:

http://ceres.larc.nasa.gov/order_data.php


Kato, S., and N. G. Loeb, 2003: Twilight irradiance reflected by the earth estimated from Clouds and the Earth's Radiant Energy System (CERES) measurements. J. Climate, 16, 2646–2650.

Kato, S., and N.G. Loeb, 2005: Top-of-atmosphere shortwave broadband observed radiance and estimated irradiance over polar regions from Clouds and the Earth's Radiant Energy System (CERES) instruments on Terra. J. Geophys. Res., 110, doi:10.1029/2004JD005308.

Loeb, N. G., K. J. Priestley, D. P. Kratz, E. B. Geier, R. N. Green, B. A. Wielicki, P. O. R. Hinton, and S. K. Nolan, 2001: Determination of unfiltered radiances from the Clouds and the Earth's Radiant Energy System (CERES) instrument. J. Appl. Meteor., 40, 822–835.

Loeb, N.G., N. M. Smith, S. Kato, W. F. Miller, S. K. Gupta, P. Minnis, and B. A. Wielicki, 2003: Angular distribution models for top-of-atmosphere radiative flux estimation from the Clouds and the Earth's Radiant Energy System instrument on the Tropical Rainfall Measuring Mission Satellite. Part I: Methodology. J. Appl. Meteor., **42**, 240–265.

Loeb, N.G., S. Kato, K. Loukachine, and N. M. Smith, 2005: Angular distribution models for top-of-atmosphere radiative flux estimation from the Clouds and the Earth's Radiant Energy System instrument on the Terra satellite. Part I: Methodology. J. Atmos. Oceanic Technol., **22**, 338–351.

Loeb, N.G., S. Kato, W. Su, T. Wong, F.G. Rose, D.R. Doelling, and J. Norris, 2011: Advances in understanding top-of-atmosphere radiation variability from satellite observations. Surveys Geophys. (submitted).

Loeb, N.G., S. Kato, K. Loukachine, and N, Manalo-Smith 2007, Angular distribution models for top-of-atmosphere radiative flux estimation from the Clouds and the Earth's Radiant Energy System instrument on the Terra satellite. Part II: Validation, J. Atmos. Oceanic Technology, 24, 564-584.

Loeb, N.G., W. Sun, W.F. Miller, K. Loukachine, and R. Davies, 2006: Fusion of CERES, MISR and MODIS measurements for top-of-atmosphere radiative flux validation, J. Geophys. Res., 111, D18209, doi:10.1029/2006JD007146.

Loeb, N.G., B.A. Wielicki, D.R. Doelling, G.L. Smith, D.F. Keyes, S. Kato, N.M. Smith, and T. Wong, 2009: Towards optimal closure of the earth's top-of-atmosphere radiation budget. J. Climate, 22, 748-766.

Loeb, N.G., S. Kato, and B.A. Wielicki, 2002: Defining top-of-atmosphere flux reference level for Earth Radiation Budget studies, J. Climate, 15, 3301-3309.

Minnis P., S. Sun-Mack, D.F. Young, P.W. Heck, D.P. Garber, Y. Chen, D.A. Spangenberg, R.F. Arduini, Q.Z. Trepte, W.L. Smith, Jr., J.K. Ayers, S.C. Gibson, W.F. Miller, V. Chakrapani, Y. Takano, K.-N. Liou, Y. Xie, 2011: CERES Edition-2 cloud property retrievals using TRMM VIRS and Terra and Aqua MODIS data, Part I: Algorithms, IEEE Trans. Geosci. and Rem. Sens. (in press).

Sun, W., N.G. Loeb, S. Kato, B. Lin, Y. Hu, and C. Lukashin, 2011: A study of subvisual clouds and their radiation effect with a synergy of CERES, MODIS, CALIPSO, AIRS, and AMSR-E data. Atmos. Chem. Phys. (submitted).

Thomas S., K.J. Priestley, N. Manalo-Smith, N.G. Loeb, P.C. Hess, M. Shankar, D.R. Walikainen, Z.P. Szewcyzk, R.S. Wilson, D.L. Cooper, 2010: Characterization of the Clouds and the Earth's Radiant Energy System (CERES) sensors on the Terra and Aqua spacecraft, Proc. SPIE, Earth Observing Systems XV, Vol. 7807, 780702, August 2010.

## 8. Revision History

[Document changes in the dataset and the technical note if a new version replaces an older version published on the ESG.]

Rev 0 – 08/09/2011 - This is a new document/dataset